Low-cost dynamic tensile testing

H. Schindler, M. Veidt

JOURNAL DE PHYSIQUE IV
Colloque C8, supplément au Journal de Physique III, Volume 4, septembre 1994

Low-cost dynamic tensile testing

H.J. Schindler and M. Veidt

Swiss Federal Laboratories for Materials Testing and Research, Section Technology of Metals/Joining, Ueberlandstr. 129, 8600 Dubendorf, Switzerland

Résumé: Cet article décrit une nouvelle méthod qui permet d'effectuer des essais de traction avec des vitesses d'allongement atteignant jusqu'à 600 s^{-1} et à différentes températures. Cette méthode consiste à soumettre une petite éprouvette de traction, montée dans une màchoire ressemblant à une éprouvette Charpy modifiée, à une sollicitation dynamique sur un mouton pendule instrumenté. Des relations cinématiques et cinétique permettent de déterminer la courbe contrainte-allongement à partir du signal de force mesuré. Les premiers résultats obtenus montrent que cette méthode est très prometteuse pour déterminer l'influence de vitesse d'allongement très élevées et de différentes températures sur les caracteristiques mécaniques des matériaux structuraux.

Abstract: This paper reports on the development and first application of a low-cost tensile test method utilizing an instrumented Charpy pendulum. It allows for simple tensile testing at increased loading rates up to 600 s^{-1} at various temperatures. The stress-strain curve is determined from the measured force history using kinematical and kinetic relations. The first results show that the new technique is very promising to determine the influence of loading rate and temperature on the mechanical properties of structural materials.

1. INTRODUCTION

To predict the mechanical behavior of structures under impact loading, the material properties should be known for the actual strain rate and temperature. However, the data reported in the literature are limited to a few of the most widely used structural materials. Determining these properties experimentally often exceeds the budget of the corresponding project, since these experiments are costly and require special testing equipment which is available only in a few laboratories, e.g. [1], [2]. So the effect of loading rate and temperature on the mechanical properties of structural materials is often left to assumptions.

The situation is different in toughness testing. Here, testing under increased loading rate and various temperature is very common, with the Charpy V-notch being one of the most widely performed tests to get information about the loading rate and temperature effect. Many material testing laboratories are equipped with an instrumented Charpy pendulum that enables them to do also more sophisticated toughness testing, e.g. [3]. In these cases the increased loading rate actually simplifies the testing equipment and procedure; the tests require neither a special displacement measuring device nor a temperature controlled environment.

These considerations led to the idea of modifying a Charpy V-notch specimen such that the tensile properties could be evaluated approximately by utilizing the instrumented Charpy pendulum, taking advantage of the simplicity of these tests. A first experimental attempt to determine dynamic stress-strain curves with specimens as shown in Fig. 1 was encouraging.

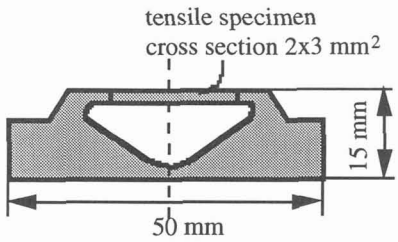

Fig. 1: Modified Charpy specimen for dynamic tensile testing.

The disadvantage of such tests was the relatively expensive machining of the specimens because of its complex shape, as well as certain waste of material in cases of shortage of testing material. Furthermore plastic hinges are formed at the ends of the tensile specimen. To overcome these drawbacks, the re-usable clamping device presented herein was developed.

2. CLAMPING DEVICE

The clamping device is shown in Fig. 2. It consists of two arms (A) which rest on the supports of the Charpy pendulum at one end and are connected to the tensile specimen (B) at the other. This end is forked in order to pull the specimen symmetrically. The connection between the fork and the tensile specimen is such that essentially only a tensile force is transmitted. This is realised by the cylindrical shoulders (C) that are connected to the threaded ends of the specimen and that are meant to glide on the contact area, causing thereby only a small frictional moment. The two arms are in touch with a central pivot (D), allowing for a rotational degree of freedom between them, thus forming a hinge-like connection.

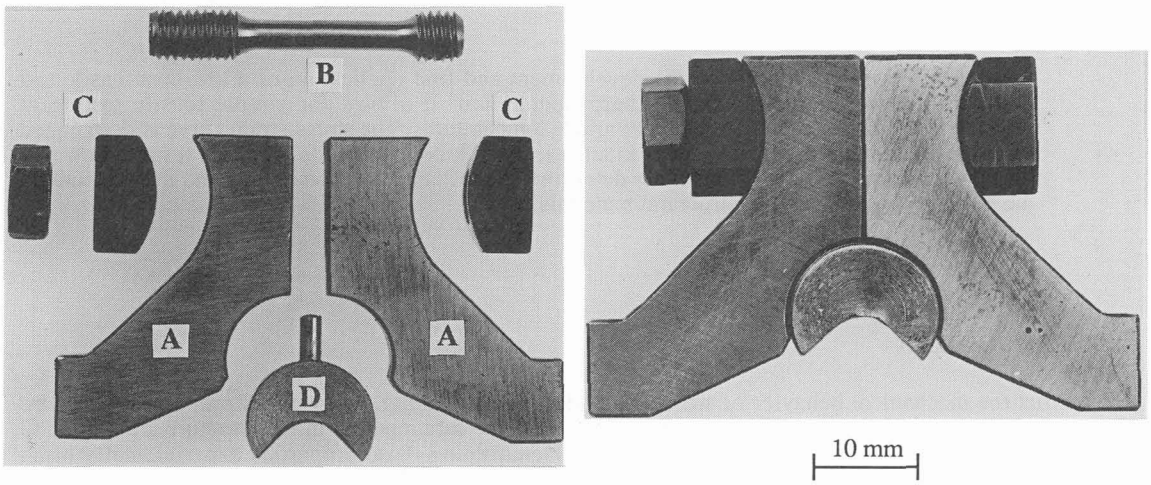

a b

Fig. 2: Clamping device for tensile tests at increased loading rates and various temperatures, a) exploded view, b) assembled view

During a test, the tup of the pendulum hammer hits the center of the pivot. The impact imposes a movement on the arms that contains a component of relative rotation centred at the pivot. Therewith the forked ends of the arms move apart from each other, stretching the small tensile specimen that is spanned between them. The loading process is visualized by the sequence of pictures shown in Fig. 3.

The instrumented pendulum hammer delivers the force $F(t)$ and the pivot displacement $s(t)$ at each moment. From these experimental data the stress-strain relation can be obtained from kinematical and kinetic relations as shown in the next chapter.

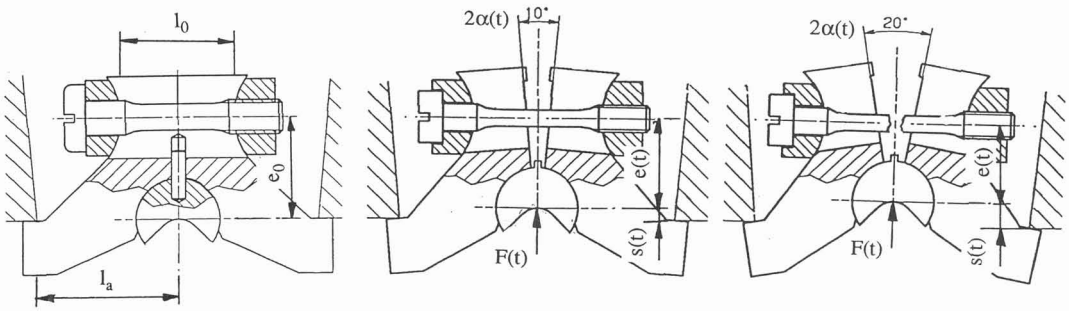

Fig. 3: Three subsequent positions of the clamping device during the loading process.

A practically important feature of the device is that all parts (A) - (D) are fixed to each other by slightly pre-stressing the tensile specimen, forming a single "rigid" body as shown in Fig. 2b. This feature is important since it makes testing at different temperatures possible by simply pre-cooling or pre-heating of the entire clamping device like a specimen in Charpy V-notch testing. Placing the device on the supports of the Charpy pendulum only needs a few seconds, so the temperature remains approximately constant.

3. ANALYSIS

From the experiments using an instrumented pendulum the force history $F(t)$ during the tearing process is known. The displacement of the pivot $s(t)$ is determined from $F(t)$ analytically by integrating Newton's law.

$$s(t) = \int_0^t \left(v_0 - \int_0^\tau \frac{F(\xi)}{m_h} d\xi \right) d\tau \qquad v_0\text{: impact velocity, } m_h\text{: mass of the pendulum} \tag{1}$$

From a given displacement $s(t)$ the position of every point of the arms and the pivot which can be considered as rigid bodies, is known as a function of time. Hence, the strain and strain rate in the specimen can be calculated. The position of the specimen with respect to the loading device is characterized by its eccentricity $e(t)$ (see Fig. 3), i.e. the distance of the specimen axis to the center of the pivot which is

$$e(t) = e_0 \cos[\alpha(t)] - \left\{ \frac{l_0}{2} + r \right\} \sin[\alpha(t)] \tag{2}$$

with e_0 denoting the initial eccentricity, l_0 the initial length of the cylindrical shaft of the specimen, r the radius of the fork and $\alpha(t) = \text{atan}[s(t)/l_a]$ the angle that describes the rotation of the arms. The length l_a is the distance from the center of strike to the anvil. The elongation $\Delta l(t)$ of the specimen that is imposed on it by the fork is correspondingly given by

$$\Delta l(t) = 2\left[e_0 \sin[\alpha(t)] + \left\{ \frac{l_0}{2} + r \right\} \cos[\alpha(t)] \right] - l_0 \tag{3}$$

Thus, the average strain in the specimen is

$$\varepsilon(t) = \frac{\Delta l(t)}{l_0} \tag{4}$$

In the plastic range the strain rate $\dot{\varepsilon}(t)$ in the specimen is calculated by differentiating (4) whereas in the elastic range it is somewhat reduced due to additional elastic effects.

The stress can be calculated from the momentum equilibrium using the measured force $F(t)$ as input signal. In its most general form a system of seven coupled, non-linear equations results that is omitted here for reasons of brevity. Ignoring friction and considering that $\alpha(t)$ is small, the simplest, quasi-static equation to determine the engineering tensile stress in the specimen becomes

$$\sigma(t) = \frac{2l_a}{\pi d_0^2 e(t)} F(t) \tag{5}$$

with d_0 being the initial diameter of the cylindrical shaft of the specimen.

It is appropriate to discuss the influence of friction by considering the energy balance. The individual terms in the global energy balance can be calculated using the kinematic relations mentioned above and the geometry and masses of the set-up. A detailed analysis shows that the dissipated energy due to the inelastic impact, the kinetic energy of the clamping device and the specimen and the elastic strain energy stored in the clamping device and the specimen can be neglected. These quantities are at least one order of magnitude smaller than the kinetic energy of the striker, the plastic work in the specimen and other dissipative sinks especially the friction between the different components of the clamping device. After plastic deformation in the specimen has started, the plastic work in the specimen W^P and the energy dissipated by friction W^f are the only two terms to be considered in an incremental energy balance.

$$\delta W(t) = F(t)\delta s = \delta W^p(t) + \delta W^f(t) \qquad \text{with} \qquad \delta W^f(t) = \mu_{eff}(t) C(s,\dot{s}) F(t) \delta s \tag{6}$$

Because the frictional forces and relative motions between the different components of the clamping device can be calculated from the kinetic and kinematical relations mentioned above, the coefficient $C(s,\dot{s})$ in (6) can be calculated and the effective frictional coefficient $\mu_{eff}(t)$ remains the only unknown in the equation for calculating W^f. Although it certainly will depend on the velocity of the relative motions between the different components of the clamping device, it can be estimated using for example values determined from static bending tests of the device.

Until necking starts the plastic work in the specimen can be calculated as

$$\delta W^p(t) = \frac{\pi d_0^2}{4} l_0 \sigma(t) \dot{\varepsilon}^p(t) \tag{7}$$

The lefthand side of (6) is delivered from the instrumentation. Thus, in the region of stable plastic straining the tensile stress $\sigma(t)$ in the specimen can be determined using equations (6) and (7).

4. EXPERIMENTS

A ductile pressure vessel steel of the type 20MnMoNi55 is used for the preliminary tests of the set-up. The shape of the specimens that are cut from a solid block are shown in Fig. 2a. From a static tensile test its ultimate tensile strength R_m and the corresponding plastic strain ε_m^p, its yield stress R_e and its plastic fracture strain ε_f^p are determined to be $R_m = 695$ N/mm^2, $\varepsilon_m^p = 5$ %, $R_e = 530$ N/mm^2 and $\varepsilon_f^p = 12.5$ %.

The dynamic experiments are performed on a Wolpert 30/15 K-E pendulum (mass $m_h = 19.7$ kg) using an instrumented DIN tup and an electronic device built by the Frauenhofer Gesellschaft für Werkstoff-mechanik in Freiburg i.Br., Germany to measure the force as a function of time and calculate on-line the velocity, displacement and dissipated energy histories. For data acquisition a transient recorder Nicolet 440 is used.

The material is tested at two impact energies, $E_0 = 150$ J and $E_0 = 50$ J and three different temperatures, -65°C, room temperature (RT) and 150°C. The strain rate right after impact is $\dot{\varepsilon}_0 \approx 380$ s^{-1} for $E_0 = 150$ J and $\dot{\varepsilon}_0 \approx 220$ s^{-1} for $E_0 = 50$ J. Its values at the beginning of the plastic instability are approximately $\dot{\varepsilon}_m \approx 310$ s^{-1} and $\dot{\varepsilon}_m \approx 190$ s^{-1}. Fig. 4a shows three typical force histories for the three temperatures tested.

Qualitatively, the force histories look similar to the signals of an instrumented Charpy test, e.g. [3]. The main difference occurs at the beginning of the signal where no distinct inertia peak is present like it is characteristic for a Charpy test. Additionally, the initial portion of the signal slightly differs from one experiment to the other. This is due to the alignment of the holder with respect to the center of impact and the fixture that is necessary to hold it in position. When the striker hits the pivot, the first thing that happens is a slight movement of the holder mainly perpendicular to the impact direction to align itself with respect to the center of strike. This approximately needs 150 µs varying from experiment to experiment. The actual tension test starts after this alignment phase. The plastic straining process lasts about 1.2 ms. After approximately 0.5 ms the point of maximum force is reached, where necking starts. Fig. 5 shows a specimen before and after testing.

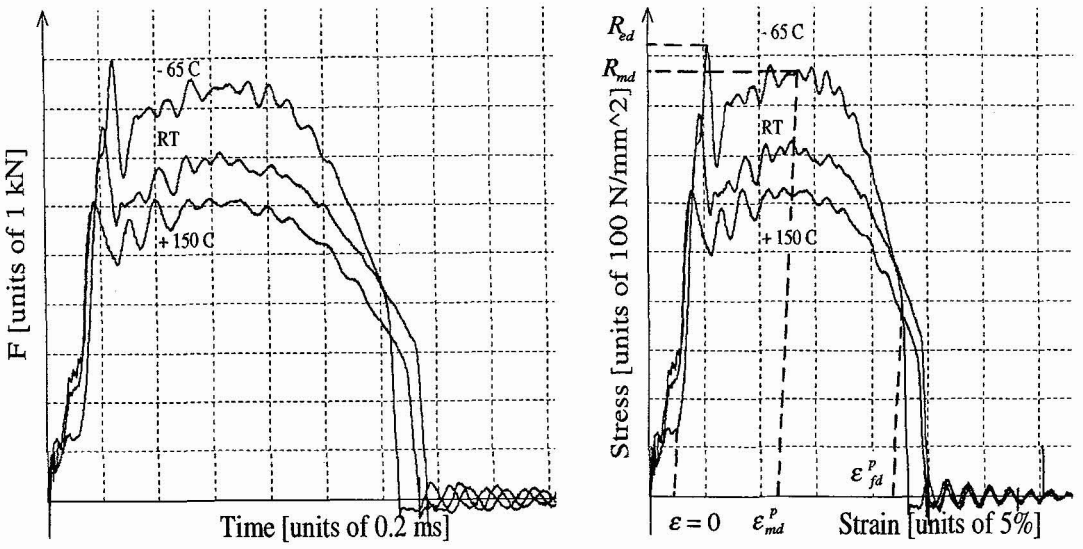

a b

Fig. 4: a) Typical $F(t)$ signals, strain rate after impact $\dot{\varepsilon}_0 \approx 220\ s^{-1}$ ($v_0 = 2.25$ m/s), strain rate at beginning of plastic instabiliy $\dot{\varepsilon}_m \approx 190\ s^{-1}$.
b) Stress-strain curves calculated from the measured $F(t)$ signals using equations (4) and (5).

Because no filtering of the raw data is used, considerable oscillations are present in the stress-strain curves in Fig. 4b. Nevertheless, the main features and quantities like the dynamic ultimate tensile strength R_{md}, the corresponding plastic strain ε^p_{md}, the dynamic elastic limit R_{ed} and the plastic strain at fracture ε^p_{fd} can be determined from the curves. These characteristic quantities are summerized in Table 1.

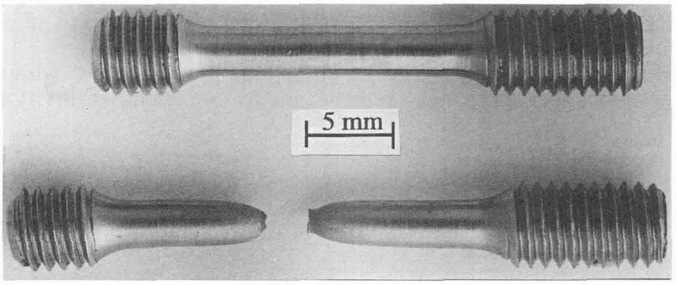

Fig. 5: Specimen before and after dynamic tensile test.

The strain values ε^p_{md} and ε^p_{fd} can also be determined by measuring the diameter and the length of the broken specimens assuming volume constance during plastic deformation. Within the accuracy of the measurement systems used to determine these quantities, they are identical for all specimens. Their mean values are determined to be $\varepsilon^p_{md} = 12$ % and $\varepsilon^p_{fd} = 24$ %. They are in good agreement with the strain values directly determined from the measured force histories.

As expected, the most pronounced influence of the increased strain rate is on the elastic limit R_e of the material. Certainly, the increase of up to 120 % compared with the static value at RT is not only a material effect, but is also due to the oscillation and friction.

Table 1: Characteristic dynamic quantities determined from measured $F(t)$ signals.

$\dot{\varepsilon}_0$ [s^{-1}]	$\dot{\varepsilon}_m$ [s^{-1}]	Temperature [C]	R_{ed} [N/mm^2]	R_{md} [N/mm^2]	ε^p_{md} [%]	ε^p_{fd} [%]
220	190	-65°	925	875	9	19
220	190	RT	790	715	9	21
220	190	150°	630	630	9	21
380	310	-65°	1225	875	10	22
380	310	RT	895	725	9	21
380	310	150°	895	655	9	22

At RT the static value of the ultimate tensile strength R_m is increased by 2.2 % for strain rates of approximately 200 s^{-1} and by 4.3 % for strain rates of approximately 350 s^{-1}. The strain rate dependency is not as pronounced as for R_e.
The temperature has almost no influence on the strains in the dynamic experiments but only on the global stress level. It seems that the generated heat during the plastic deformation is an important parameter. With equations (6) and (7) all the dissipative terms in the energy balance can be calculated. This allows to quantify the heat generated during the plastic straining process and it might be very interesting to analyze the effects resulting from the increased temperature in the specimen.
Temperature effects might be the reason for the larger strains that occur in the dynamic experiments compared to the static ones. The dynamic plastic strain at ultimate tensile strength ε^p_{md} and the dynamic plastic strain at fracture ε^p_{fd} are approximately 80 % larger than the same quantities in a static experiment.

5. CONCLUSIONS

The preliminary tests with the newly developed clamping device are very promising. The measured dynamic tensile properties are plausible and compare well with those obtained by "classical" techniques, [4], indicating that friction does not play a major role. The re-usable clamping device enables one to perform low-cost, dynamic tensile tests at various loading rates and temperatures. The accuracy and reproducibility of the test results seem to be sufficient for many practical applications. By using different initial impact energies, different eccentricities of the clamping device and different specimen lengths, the strain rate can be chosen in the range $50s^{-1} < \dot{\varepsilon} < 600s^{-1}$.

However, there are several aspects that need further investigation. To be mentioned among them are the effect of the friction, the interpretation of the load signal in the elastic region and near the yield point, where oscillations are present and the effect of adiabatic heating.
Most of these questions will probably be clarified by comparing the test results with the ones of static or independent dynamic tests, by direct strain measurements and by numerical sensitivity studies.

References

[1] Nicholas T. and Bless S.J., High strain rate tension testing, in Metals Handbook Ninth Edition, Vol. 8, ASM: Metals Park, (1985).
[2] Lindholm U.S., High strain rate tests, in Measurement of Mechanical Properties, Vol. 5, Part 1, R.F. Bunshah ed., Interscience Publ.: New York, (1971).
[3] ESIS TC5, Proposed standard method for the instrumented Charpy-V impact test on metallic materials, (1994).
[4] MacGillivray H.J. and Klenk A., High-rate tensile testing - progress towards a standard method, to be presented at the International Congress on Material Testing, Palaton, Hungary, (1994).

Acknowledgement

This paper was prepared in the course of research and development sponsored by the EMPA (project #132'163). The authors wish to express their thanks to O. Dambach for drawing the clamping device and Dr. R. Huwiler for the many useful discussions on instrumented Charpy tests.